PHYSICAL REVIEW B

CONDENSED MATTER

THIRD SERIES, VOLUME 35, NUMBER 17 15 JUNE 1987-I

Surface-plasmon-enhanced Brillouin scattering on silver films: Double-resonance effect

W. M. Robertson, A. L. Moretti,* and Ralph Bray
Department of Physics, Purdue University, West Lafayette, Indiana 47907
(Received 8 December 1986)

We report a continuation of our investigation of surface-plasmon-induced enhancement of Brillouin scattering of thermal surface acoustic waves of thin silver films. The experiments were performed in a Kretschmann attenuated-total-reflection configuration. In the backscattering mode, the surface plasmons are resonantly involved both in the incident and scattered radiation. The scattered radiation appears on the surface of a cone defined by the resonant interaction angle and contains Brillouin couplets, which are analyzed by a five-pass Fabry-Perot interferometer. The enhancement factor is determined from the ratio of the peak radiation on this cone to the Brillouin scattered radiation in an external reflection configuration not involving surface plasmons. The theory and experiment agree in that the double resonance gives a much larger enhancement than does the singly resonant process, which was observed in our earlier investigation for the forward-scattering configuration. The enhancement factor observed, 750 (±25%), is very dependent on the imaginary part of the dielectric constant of the Ag film, which is determined experimentally for our film as $-9.0+i0.57$. Finally, we contrast the results of our Brillouin scattering experiment with those of Raman scattering from chemical adsorbates.

I. INTRODUCTION

Nonlinear-optical phenomena occurring at surfaces of metals such as Ag are greatly enhanced when surface plasmons (SP's) are employed as intermediate agents in the interaction. SP's may appear in the form of propagating polaritons on smooth surfaces or as localized resonances on rough surfaces. In both cases, the enhancement is due to the elevated electric fields associated with SP's, which are peaked at the metal surface where the optical interaction of interest is located. Large enhancements have been observed in various surface phenomena, e.g., Raman scattering from monolayers of chemical adsorbates (known as surface-enhanced Raman scattering[1] or SERS) and second-harmonic generation (SHG).[2] There may also be a contribution to the enhancement from "chemical" effects[1] relating to the presence of adsorbed chemical species. The latter are necessarily involved in the case of SERS, and can be optionally involved for SHG.[3] Discrimination between the electromagnetic and chemical contributions is difficult, and there does not appear to be a consensus on their relative magnitude.

Our interest in the present work, as in our earlier paper[4] (hereafter referred to as MRFB), is in the analysis of a situation where the enhancement is due purely to the SP's. Such a situation is obtainable for Brillouin scattering from the thermal acoustic waves of a thin Ag film deposited on a glass substrate. The SP's serve as an intermediary in this interaction. In our experiments they are generated with the aid of the attenuated-total-reflection (ATR) Kretschmann configuration. Here, light incident on the glass prism side of a prism-metal film-air configuration generates SP's on the metal-air interface. The Brillouin interaction occurs between the SP's, whose electric fields are peaked at the Ag-air interface, and the ripples[5,6] generated on the same surface by the thermal acoustic waves characteristic of the Ag film and the glass substrate.

Brillouin scattering offers both a unique advantage and a serious limitation in analyzing the role of SP's in the enhancement of nonlinear optical phenomena. The absence of chemical effects in the interaction permits one to isolate and determine the SP (electromagnetic) contribution to the enhancement. A limitation is that Brillouin scattering studies are restricted to metal surfaces that are sufficiently *smooth* so that the SP's appear only as propagating modes with well-defined wave vector in the surface. This property is a necessary condition for observing *well-defined (sharp line) Brillouin scattering spectra.* As discussed in MRFB, the latter cannot be obtained for the case of "island" metal films or electrochemically roughened surfaces, which involve localized SP's and much large enhancements.

The Brillouin scattering interaction between propaga-

ting SP's and thermal acoustic waves of the metal film can take several different forms for which the magnitude of the SP enhancement can vary greatly. In our previous work (MRFB), we utilized a forward scattering configuration, referred to as case (2), for which the Brillouin scattered light appeared on the air side of the metal film. In the present paper we deal with the backscattering configuration [described as case (1) in MRFB], for which the scattered light is analyzed after it passes back through the glass prism. This case involves a double SP-resonant interaction and gives a much stronger SP enhancement, but it is much more difficult to carry out experimentally. Both cases involve the emission or absorption of phonons by the SP's, which eventually shows up as Brillouin shifted couplets in the analysis of the scattered electromagnetic radiation. A comparison of the two cases brings out some interesting differences in the details of the phenomena observed and of the experimental and analytical problems encountered. From this comparison we are able to demonstrate that the magnitude of the SP enhancement is much greater in case (1), in agreement with theoretical analysis. Finally, we compare our results with those of Raman scattering for thin films and demonstrate why the Brillouin scattering approach is better for analyzing the SP enhancement.

II. SP GENERATION AND THE ACOUSTIC PHONON INTERACTION; COMPARISON OF CASES 1 AND 2

As in our previous work, the Brillouin scattering studies were carried out with "smooth," thin Ag films, vacuum evaporated onto the flat, polished face of a Pyrex hemisphere (refractive index $n=1.47$), as illustrated in Fig. 1(a). The film thickness in the present experiments was 437 Å, chosen for optimum SP generation efficiency. A computer-stabilized, five-pass Fabry-Perot interferometer was used to analyze the scattered electromagnetic radiation and extract the Brillouin spectra. For further experimental details, we refer to MRFB.

The SP-phonon scattering interaction of case (1) is illustrated in Fig. 1. We analyze the sequential steps of the generation of SP's by the ATR Kretschmann method, their scattering by phonons of the Ag film, and finally their reemission through the glass as light.

(1) An Ar^+-ion-laser beam I_i at 4880 Å is incident through the glass hemisphere and focused at the glass-Ag interface. At incident angles greater than that for total internal reflection, the evanescent fields of the light penetrate through the Ag film to the metal-air face. Coupling between these fields and SP's on the Ag-air interface occurs when the light is incident at the resonant angle θ_{SP}. The resonance corresponds to the condition for the conservation of energy and of surface components of the wave vectors in the conversion from incident light to SP's. This condition is represented in Fig. 1(b) by the crossing of the light line in the prism with the dispersion curve ω_{SP} versus k_{SP} for the SP's on the metal-air interface. The wave vector of the SP's, k_{SP}, lies in the surface of the metal and is well defined. The light line in glass represents ω versus nk_x for some fixed angle of incidence; ω is the frequency, and $nk_x = nk_i \sin\theta_i$ is the surface component of the wave vector of the incident light inside the glass hemisphere with refractive index n. Thus at resonance,

$$\omega_i = \omega_{SP} \quad \text{and} \quad nk_x = k_{SP} .$$

Without the increase in k_i by the factor $n > 1$ of the glass, the incident light line could be, at most (for grazing in-

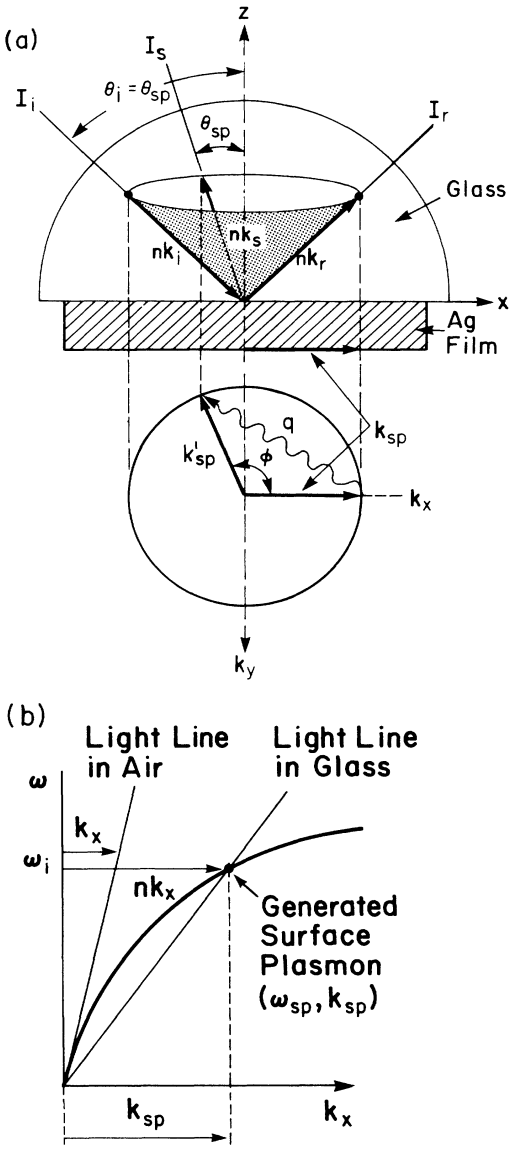

FIG. 1. (a) Kretschmann configuration used to generate the SP's, and the wave-vector diagram illustrating the scattering of an initially generated SP ($\mathbf{k}_{SP}$) through an angle ϕ into a second SP ($\mathbf{k}'_{SP}$). Scattering by a thermal distribution of surface acoustic waves leads to randomization of the SP wave vectors, and Brillouin signals that exit the glass hemisphere on the shell of a cone as indicated in the figure. (b) Dispersion curve for SP's at a metal-air interface illustrating the need for an increase in wave vector by a factor of n (refractive index of the hemisphere) to permit coupling of light to the SP's.

cidence), only parallel to the base of the SP dispersion curve and the light could not couple to the SP's.

The resonant generation of SP's at the Ag-air interface occurs at the expense of the intensity of the reflected light beam I_r, which undergoes a sharp decrease from almost 100% to $\sim 5\%$.[4] The resonant angle θ_{SP}, is determined by the real part of the wavelength-dependent dielectric constant of the Ag film and the half-width of the resonance by the imaginary part. A further important point is that the electric fields of the SP's lie in the plane perpendicular to the surface of excitation, and thus SP's can only be generated by p-polarized light. The fact that the efficiency of the SP generation process can be controlled by varying the polarization of the incident light proved to be very useful as shall be demonstrated.

(2) When a SP is scattered by an acoustic phonon of the film, through an angle ϕ, the scattered SP wave vector $\mathbf{k}'_{SP}$, is related to the original SP wave vector $\mathbf{k}_{SP}$, and the phonon wave vector $\mathbf{q}$, by the relation,

$$\mathbf{k}'_{SP}=\mathbf{k}_{SP}\pm\mathbf{q} .$$

The corresponding frequencies are related by the equation,

$$\omega'_{SP}=\omega_{SP}\pm\omega(q) ,$$

where $\omega(q)$, the frequency of the acoustic phonons, is much less than ω_{SP}. The frequency shifts of the scattered SP's ultimately form the Brillouin couplets. The three wave vectors involved in the scattering process lie in the plane of the Ag-air boundary. Since the scattering is by a thermal equilibrium distribution of phonons, the scattered SP's have wave vectors which are randomized. As illustrated in Fig. 1(a), they must lie on a circle of constant k, since the energy gain (loss) in the phonon absorption (emission) processes is negligible.

(3) Because the magnitude of the SP wave vectors is unchanged, the randomly scattered SP's can all couple back as light passing through the glass at the same resonant angle θ_{SP}. As a result, the electromagnetic radiation that emanates through the glass hemisphere lies on the shell of a cone of angle θ_{SP}, as shown by the shading in Fig. 1(a). It can be observed to project as a sharp circle of light on a screen held above the hemisphere. In Fig. 2, we show photographs of such projections, with front and side views, taken from a screen with two holes punched through it to transmit the much more intense incident and reflected laser beams. The glass hemisphere and silver film are also visible in the photographs. The circle of light is direct evidence of the randomization of the generated SP's before they couple out. However, the intensity of the projected circle of light is much too great to be due to the SP scattering by the phonons alone. Most of it is elastic Rayleigh scattering due to the inherent defects or roughness of the Ag film. Such an experimental arrangement has been used before[7,8] for analyzing the Fourier components of the surface roughness. Our interest, however, is limited to the phonon-induced contribution to the

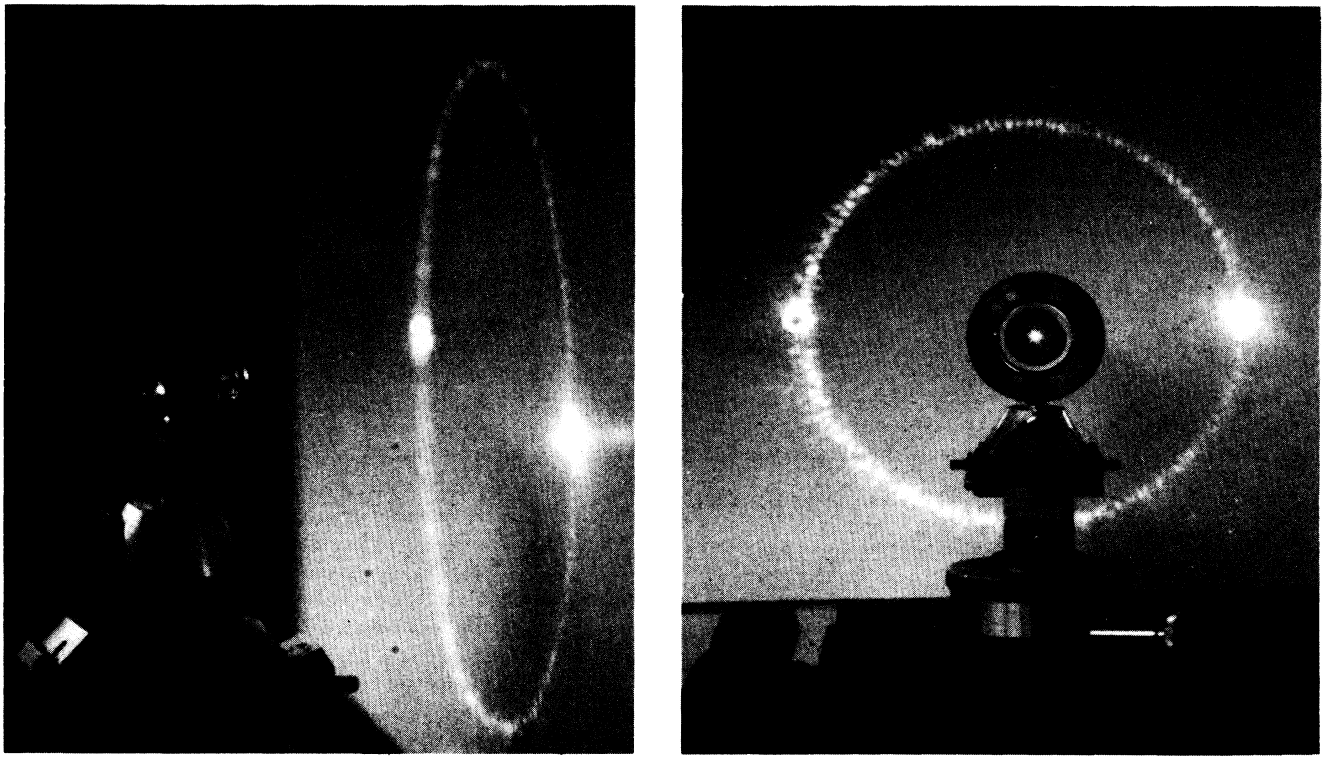

FIG. 2. Photographs with front and side views of the experimental configuration showing the ring of light projected on a screen; the ring is due to SP wave-vector randomization by scattering in the Ag film and subsequent reradiation through the glass via prism coupling.

scattered light. To extract this information the light on any portion of the circle must be analyzed with a Fabry-Perot interferometer.

We note the significance of the fact that we do observe sharp-line Brillouin couplets for the light scattered out either on the air side (see MRFB) or on the cone through the glass analyzed here. These signals must have originated from phonon interactions with the well-oriented, originally generated SP's and not the randomized SP's. The latter would give rise to a continuum rather than a sharp-line Brillouin spectrum. This indicates the dominance of the well-oriented SP's over the randomized SP's and we can conclude that the rate of SP randomization by phonons and roughness is weak compared to the rate of SP attenuation by all other processes. A similar conclusion could have been drawn from a comparison of the weak integrated intensity on the ring ($\sim 0.1\%$) (Ref. 9) to the incident intensity.

The analysis of the Brillouin spectrum in this configuration turned out to be more difficult than anticipated. The complication is due to undesired Brillouin scattering contributions arising from the bulk phonons of the glass. These contributions originate in the focused volume of the beam at the glass-Ag interface. Two separate Brillouin couplets are generated there, one from the incident and another from the reflected beam. These contributions have nothing to do with the SP's and are not restricted to the surface of the cone of light emanating from the glass hemisphere. How we identified and eliminated these undesired contributions will be described in Sec. III.

With the help of Fig. 3 we next contrast the back-scattering of case (1) and the forward scattering of case (2). The generation of SP's is identical; it occurs when the incident light line in the glass crosses the SP dispersion curve in Fig. 3. If the subsequent interaction with phonons generates a SP with wave vector terminating on the circle of constant k_{SP}, then we have case (1), i.e., the scattering of one SP to another which can ultimately convert to light which is emitted on the shell of a cone through the glass hemisphere. However, the scattered wave vector can also terminate at any point *within* the circle, as illustrated in Fig. 3. In that case, it lies on some light line in air, and it can appear as "forward" scattered light within the half-solid angle on the air side of the film. Here, the phonon scattering process has aided in the coupling out of the SP as light. The equations for conservation of energy and of wave vector in the surface, governing the last case are given by

$$\omega' = \omega_{SP} \pm \omega(q) \quad \text{and} \quad k_x' = k_{SP} \pm q \ ,$$

where now ω' and k' refer to the scattered photon in air, which takes on whatever wave vector component perpendicular to the surface k_z', necessary to satisfy the relationship,

$$(\omega')^2 = c^2[(k')_z^2 + (k')_x^2] \ ,$$

where c is the velocity of light in air. The inelastic Brillouin components are again obscured by a much stronger elastic contribution from surface defects, and the two must be separated by the Fabry-Perot interferometer.

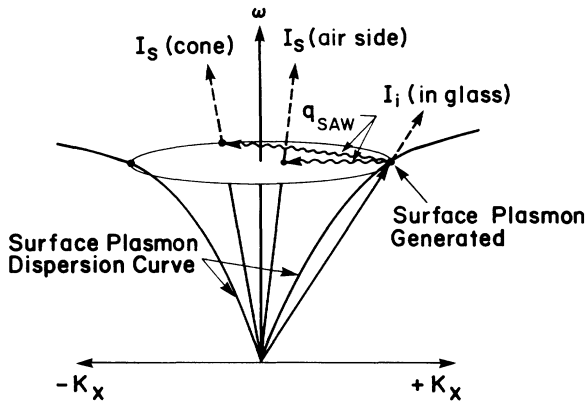

FIG. 3. Dispersion curve of SP's illustrating the two possible Brillouin scattering processes for a SP generated by light incident through the hemisphere. The interaction with a surface acoustic wave can scatter the SP either directly into light on the air side [case (2)] or into a second SP which can then radiate out as light on the cone on the glass side [case (1)].

A phonon-assisted coupling of SP's into light, similar to that discussed in case (2) above, can also take place on the glass side of the Ag film. However, the light generated in this process would have to pass *nonresonantly* from the Ag-air interface through the Ag film to the glass side and it would be very greatly attenuated in the process.

In comparing the scattered light observed in cases (1) and (2), we have to keep in mind that: (a) different phonons in the Ag film are involved, and (b) the filling of the collection lens by the scattered light will be very different. In case (2) the scattered light can fill the whole collection lens, whereas in case (1) it is restricted to a very thin strip, a segment from the ring. Taking this difference into account is very important in comparing the SP enhancement factor for the two cases (see Sec. IV).

III. EXPERIMENTAL RESULTS

A. Analysis of the Brillouin spectra

The analysis of the Brillouin spectrum for the light scattered on the ring requires that we distinguish the SP-enhanced signals of the metal-film from the undesired bulk phonon couplets generated in the glass. The frequency shifts associated with the latter (22 and 31 GHz), are much larger than those arising from the metal film (e.g., 6.4 GHz at $\phi = 120°$). In a tandem Fabry-Perot interferometer such very different frequencies would appear well separated and distinguishable. However, in the absence of the tandem feature in our five-pass interferometer, the orders overlap, and it can be difficult to identify the different spectral contributions. The problem was solved in the following manner.

With the mirror spacing of the interferometer adjusted for large free spectral range (FSR), we could identify and measure the higher frequency Brillouin signals from the glass hemisphere itself. For this FSR, the low-frequency signals from the phonons of the Ag film were hidden

within the very strong Rayleigh peaks. We then attempted to reduce the FSR to a value which was both convenient for looking at the ~6-GHz signal from the Ag film, and also was close to submultiplets of both of the higher frequency bulk Brillouin couplets. The objective was to hide the bulk phonon signals from the spectrum by burying them in the Rayleigh peaks. We could achieve this occasionally, but in general it is difficult to bury both phonon couplets. However, it was fairly easy to bury one of the couplets, and we preferentially selected the one from the incident laser beam. We could then dispose of the remaining couplet from the reflected beam by exploiting the special dependence of the reflectivity on the polarization of the incident light. This technique is illustrated in the interferometer spectra in Fig. 4. Here, the bulk phonon peaks due to the incident light are already buried in the Rayleigh peak. With *s*-polarized light incident through the hemisphere at θ_{SP}, SP's are not generated, and there is no signal in Fig. 4(a) from the phonons of the Ag film. The one observable couplet represents the Brillouin scattering of the reflected beam by bulk phonons in the glass. Figure 4(b) demonstrates the effect of rotating the polarizer in the incident beam partially towards *p* polarization. A film signal now appears at 6.4 GHz; it is stronger than the bulk phonon signal which has weakened appreciably. Finally, in Fig. 4(c), for pure *p*-polarized light, the bulk phonon signal from the glass has disappeared completely, leaving only a very strong film signal. Note that the data in Fig. 4(a) and 4(b) were multiplied by a factor of 10. The controlled onset of the SP-enhanced signal from the phonons of the Ag film represents the dependence of SP generation on the degree of *p* polarization of the incident light. The disappearance of the bulk phonon peaks is due to the decrease in the reflected light intensity which is associated with the optimization of the generation of SP's. It can be seen that the film signal becomes much stronger than the bulk phonon peak for *s*-polarized light. Thus, the usual dominance of bulk scattering (with its larger interaction volume) over surface scattering has been reversed here for the case of resonant SP generation.

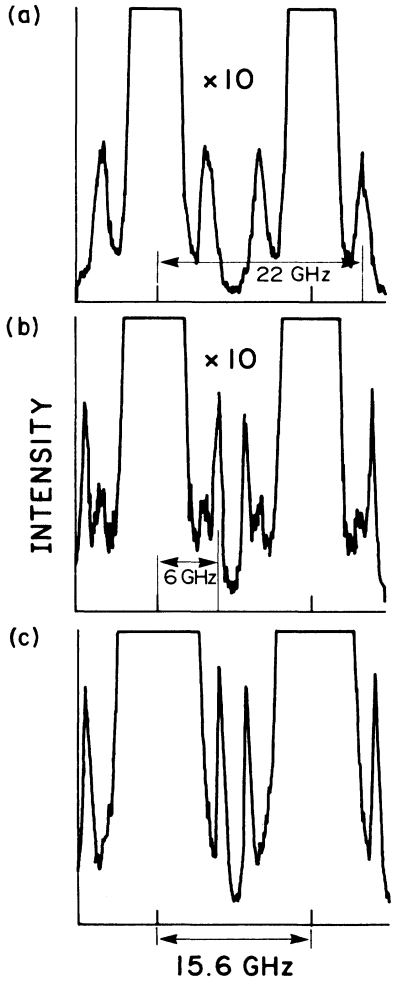

FIG. 4. Fabry-Perot interferometer spectra of light collected from the ring and its vicinity for three different incident light polarizations. Two orders appear in each spectrum; the large truncated peaks are due to the elastically scattered light. The light was incident in each case at θ_{SP}, but its polarization was varied as follows. In (a), it was *s* polarized and we obtained only the bulk phonon couplet at ±22 GHz. In (b), the polarization was rotated 20° from *s* polarized. The bulk phonon peaks are partially suppressed and are in fact exceeded by the surface phonon couplet at ±6 GHz. In (c), where the light is *p* polarized, the bulk phonon contribution is completely suppressed and the surface phonon peaks rise to their maximum intensity.

B. Experimental determination of the enhancement factor

To establish the magnitude of the SP-enhancement factor we need to compare the peak intensity of Brillouin scattered light on the ring with that obtained in a configuration in which SP's are not involved. Our objective is to determine the enhancement due solely to the involvement of the SP's. We tested a number of configurations for comparing the resonant and nonresonant signals. It is difficult to find a configuration in which nothing changes except the SP involvement. For each option we considered, there were several other factors which could also affect the measurements. In this section we identify these factors and discuss the experimental difficulties encountered for each option. For the option which we finally adopted, we analyze the specific corrections that need to be made for the extraneous factors in obtaining our measured value for the SP enhancement.

(a) SP generation can be controlled by varying the polarization of the incident light. Without any change in the optical configuration for collection and analysis of the Brillouin scattered light, we can compare the scattered light intensities for *p*- and *s*-polarized incident light. The advantage of this method is that the incident and scattered angles are unchanged, and there is no need to realign the optics. The disadvantages are that the nonresonant scattering intensity is due to the phonon ripples on the glass-Ag interface instead of the Ag-air interface, and the polarization of the incident light is different. However, before analyzing the effect of these factors we gave up on this approach because of some practical difficulties. With

the incident s-polarized light, there was a very weak residual "ring" of light radiating from the hemisphere, indicating that SP involvement was not completely eliminated. In spite of this residual effect the Brillouin signals were difficult to discern and analyze; they were superimposed on a large background, possibly from fluorescence in the glass.

(b) A second approach to controlling the SP involvement is based on tuning both the incident and scattered angles from on- to off-resonance values. The unenhanced Brillouin signals thus obtained again originate predominantly from the ripples on the glass-Ag interface. Experimentally implementing this approach also proved to be too difficult. As in (a), the off-resonant signals could be barely discerned against a large background. This pervasive difficulty led us to conclude that it was inadvisable to measure the off-resonant signal on the glass side, and forced us to adopt option (c).

(c) To obtain a signal free of SP involvement we resorted to the external reflection (ER) configuration, in which the light is both incident and scattered on the air side in the plane of the incident and reflected light as in MRFB. This technique has several advantages. The signal is observed from the phonons on the Ag-air interface, as in the resonant case. Also, well-defined Brillouin signals can be seen without any of the experimental problems described in (a) or (b). However, this approach is not without several drawbacks. These will be identified below in conjunction with the presentation of the data.

In Fig. 5 we compare Fabry-Perot interferometer scans for a SP-enhanced spectrum obtained from a segment of the ring [Fig. 5(a)] with an unenhanced spectrum obtained in the ER configuration [Fig. 5(b)]. The same collection lens (1-cm diameter, focal length 2.5 cm) was used for both of these cases. The resonant scattering was measured for SP's scattered through an angle $\phi = 120°$, and emerging on the ring with $\theta_{SP} = 46.3°$. The ER measurement was performed with incident angle $\theta_i = 69°$ and scattered angle $\theta_s = 23°$, as in Fig. 2(b) of MRFB. After correction for the different laser intensities used in obtaining the two scans, the Brillouin signal in the ring case is ~ 55 times stronger than in the ER case. The power that could be used in the resonant case is limited because the Ag film is susceptible to damage by the intense SP generation.

It is important to note that the ratio of fifty-five is not yet a valid measure of the enhancement; it requires several further corrections. An essential correction to the "raw" data must be made for the different spatial distribution of the scattered light in the two measurements. In the ER case, as in any nonresonant measurement, the Brillouin scattered light uniformly fills the collection lens, whereas in the ring case the Brillouin signal of interest is contained only in the very narrow segment of the ring falling on a similar collection lens. This difference makes the SP enhancement factor dependent on the size of the collection aperture used. It is meaningless to define the enhancement except in terms of the peak intensity within the width of the ring itself. This is the definition employed in the theoretical analyses which will be discussed in the next section. To measure this peak intensity experimentally we used a narrow slit in the resonant case to restrict the light as nearly as possible to the most intense portion of the ring.

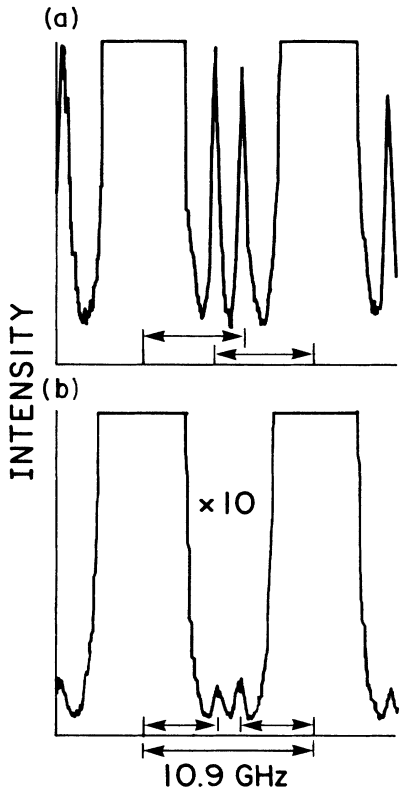

FIG. 5. Fabry-Perot interferometer spectra showing (a) enhanced Brillouin scattering for light on the ring and (b) unenhanced scattering in the ER configuration. The spectra were taken with the same size collection apertures and have been normalized for the different powers used in each case. The relevant frequency shifts of the Brillouin peaks are indicated in the figure. Note that in (a) the Brillouin peaks are overlapped in the spectrum.

We scanned the ring width with a variety of slits and found that the narrowest feasible slit size we could use was 0.25×2 mm.[2] At smaller slit widths the signal decreases disproportionately. We attributed this effect to the increase in the divergence of the scattered light beam because of diffraction at the slit. Fabry-Perot interferometer operation, particularly in the five-pass mode, is very sensitive to angular divergence of the input light. To obtain a signal of reasonable magnitude for the much weaker scattered light in the ER configuration, we used a much larger (circular) aperture of 4-mm diameter.

With the apertures indicated we repeated the Brillouin scattering measurements eight times, going back and forth between the two configurations. We obtained a value of 15 ($\pm 25\%$) for the ratio of the resonant to nonresonant signals. Correcting this measured ratio for the area difference of ~ 25 in the collection apertures raises the enhancement factor to 375 ($\pm 25\%$). The large fluctuation in these measurements indicates the difficulty of reproducibly aligning the optics and the interferometer.

A further correction is required to take into account the different phonon frequencies involved in the resonant and nonresonant measurements. It is not feasible in the ER case to observe scattering from the same phonons as are used in the ring case. The phonon frequency in the resonant case is larger because of the factor of $n=1.47$ (refractive index) increase in the wave vector of the incident and scattered light on the glass side. From the spectra of Fig. 5, the phonon frequencies for the resonant and ER signals are 6.4 and 4.5 GHz, respectively. Note that in these spectra the resonant signals are overlapped but the nonresonant signals are not. The Brillouin scattered intensity is proportional to the square of the ripple amplitude,[6] and for a thermal distribution of phonons, the ripple amplitude will be inversely proportional to the frequency. Therefore, a further correction for the phonon frequency difference of a factor of $6.4^2/4.5^2=2$ is necessary, which raises the enhancement factor to 750 ($\pm 25\%$).

Finally, we caution that this value of the enhancement factor applies only for the specific scattering angles at which the unenhanced ER and enhanced ring measurements were carried out. Both of the measurements may be dependent on their respective scattering angles. However, it was not feasible for us to study the angular dependence of light scattering on the ring because of the difficulty in reproducibly realigning the optics for each scattering angle.

The enhancement by a factor of 750 for the backscattering geometry [case (1)] greatly exceeds the factor of 25 determined in MRFB for the forward scattering geometry of case (2). This demonstrates that the enhancement is much greater when the resonant SP interaction is involved in both the incident and scattered beams. However, the stronger enhancement for case (1) is only fully realizable for the peak scattered light near the center of the width of the ring.

IV. THEORETICAL ANALYSIS OF THE ENHANCEMENT FACTOR: COMPARISON WITH EXPERIMENT

A. Introduction

We have discussed how the experimental means of determining the SP-enhancement factor for case (1) were limited by practical considerations. The available theoretical analyses of SP-enhancement are also limited in their scope. They have been formulated for scattering of light in the plane defined by the incident and reflected beams. For such in-plane scattering, the fully resonant scattering case occurs only when the light is incident and scattered at θ_{SP}. This corresponds to the backscattering of the SP's generated in the Ag film [$\phi=180°$ in Fig. 1(a)]. The theory has not been developed for the case of scattering on the ring at arbitrary angles ϕ, including the angle $\phi=120°$ case used in our experiment. Our discussion below is limited to in-plane scattering. In spite of this restriction the existing theory is still very useful for revealing some interesting features of resonant scattering.

The first theoretical analysis for in-plane Brillouin scattering in the Kretschmann configuration was reported by Fukui *et al.*[10] It applied to a thermal distribution of both bulk and surface phonons in the Ag film. For our purpose it was simpler and quite sufficient to calculate the Brillouin scattering strength for surface ripples of arbitrary amplitude following an analysis of Marvin *et al.*[11] This approach entails the solution of Maxwell's equations with optical boundary conditions imposed at the two interfaces of the Ag film which are taken to be rippled to simulate the acoustic waves. The properties of the SP's are determined by the dielectric constants of the Ag film and the glass at the applicable wavelength of light. The SP interaction with the rippled interfaces automatically gives Brillouin scattering, including interference effects between signals from the two surfaces. The intensity of the Brillouin scattering is determined by the square of the amplitude of the surface ripples due to the acoustic waves and angular factors depending on the scattering direction. The ripple amplitudes, which are arbitrary in this analysis, need not be known since in the calculation of the resonant enhancement factor the dependence on ripple amplitude cancels out. In the analysis, the ripple amplitudes on the Ag glass and Ag-air surfaces were taken to be equal.[4]

B. Application of the theory

Numerical calculations were used to determine the enhancement factor and its dependence on the dielectric constant and thickness of the Ag film. Our analysis showed that there is a much greater enhancement for case (1) than for case (2), in agreement with experiment. We also analyzed some of the pitfalls in obtaining the theoretical enhancement factor such as the interference effect between the Brillouin scattering contributions from the two sides of the Ag film.

Several features of the resonant enhancement for the backscattering configuration are demonstrated in Fig. 6, where the scattering intensity is plotted as a function of the incident angle θ_i, with the condition $\theta_i-\theta_s=0$ (i.e., for 180° backscattering of the light). The frequency of the phonons probed changes as a function of the incident angle. However, by arbitrarily keeping the ripple amplitudes constant for all phonon frequencies in our calculation, we eliminate this variable in the analysis of the resonant enhancement factor.

The backscattered Brillouin intensity in Fig. 6(a) rises to an enormous peak at $\theta_i=\theta_{SP}$; this is associated with the resonant generation and scattering of the SP's at the Ag-air boundary. To observe the much weaker off-resonant behavior, the data is replotted in Fig. 6(b) with the vertical scale expanded by a factor of 100. For θ_i far from θ_{SP} the scattering strength is due predominantly to ripples at the Ag-glass boundary and changes slowly and monotonically. The scattering contribution from the ripples at the Ag-air interface is negligible because the light is greatly attenuated in passing twice through the Ag film. However, closer to the resonant condition, the contribution from the Ag-air interface grows rapidly and begins to interfere effectively with the Ag-glass contribution. The pronounced minima in the Brillouin scattered intensity are indicative of destructive interference on both sides of the

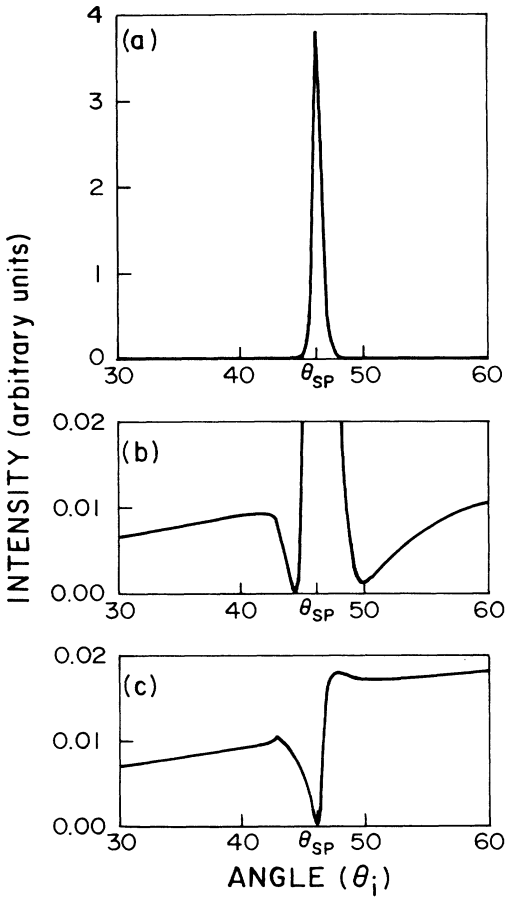

FIG. 6. Plot of the theoretically calculated Brillouin scattered intensity as a function of incident angle. All calculations were made with $\theta_i - \theta_s = 0$, i.e., 180° backscattering of light. (a) Scattering intensity with equal ripple amplitudes on both interfaces. The large peak corresponds to the enhancement due to the double involvement of SP's when $\theta_i = \theta_s = \theta_{SP}$. (b) Same spectrum as (a) but with the scale expanded to show the structure of the weak off-resonant intensities. The minima represent destructive interference of Brillouin signals from the two sides of the Ag film. (c) With the ripple amplitude set equal to zero on the metal-air interface the interference effect disappears. The minimum at θ_{SP} is due to SP generation (see text).

resonance between the Brillouin signals originating from the ripples at the two boundaries. To verify that the minima were indeed due to interference we repeated the calculation for the simulated condition of zero ripple amplitude on the Ag-air interface. The result, as plotted in Fig. 6(c), shows the disappearance of the minima and demonstrates that they indeed originated from an interference effect. The single minimum that now appears at θ_{SP} can be attributed to channeling of the incident light into SP generation at the Ag-air surface. This kills the Brillouin scattering on the Ag-glass surface. However, this minimum can be made to disappear if, instead of killing the ripple at the Ag-air face, the film is made so thick that the generation of SP's is suppressed.

If we define the enhancement factor as in approach (b), described in Sec. III B, it is obviously necessary to take the interference effects into account in arriving at a value for the enhancement factor. We should compare the peak at resonance to the off-resonant plateau in Fig. 6(b). The off-resonant value should be determined at an angle that minimizes the interference effects, preferably at $\theta_i < \theta_{SP}$ where the distorting effects of interference disappear more rapidly than for $\theta_i > \theta_{SP}$.

C. Calculation of enhancement factor

The data plotted in Fig. 6 were calculated for our experimental parameters: Ag film thickness equal to 437 Å, incident light at 4880 Å, and dielectric constant $\epsilon_{Ag} = -9.0 + i0.57$. The latter was determined specifically for our film by fitting the angular dependence of the resonance in the reflectivity as in MRFB. From the plot we obtained a value for the enhancement factor of 415 for approach (b). We compared resonant scattering from ripples on the Ag-air interface with nonresonant scattering on the Ag-glass interface. For this purpose it was obviously important to assume equal amplitudes for the ripples at each interface which is an assumption justified in MRFB. Here the nonresonant value was taken at $\theta_i = \theta_s = 42°$ where the interference effects play a negligible role. We repeated this calculation with the parameters used by Fukui *et al.* for dielectric constant ($\epsilon = -16.34 + i0.144$), incident wavelength (5145 Å) and film thickness (400 Å). This gave an enhancement factor of 7000. This order of magnitude increase illustrates the sensitivity of the enhancement to the parameters chosen for the Ag film, and emphasizes the need to determine ϵ_{Ag} experimentally for any valid comparison of theory and experiment.

We found the imaginary part of the dielectric constant to vary over a considerable range both in the literature and in our own experiments with different films. The surface quality of the film can vary widely depending on the age of the film, the method of its production, and its exposure to air. It is evident that there is no unique value that can characterize the enhancement factor.

As indicated in the previous section, approach (b) was not feasible experimentally. To more closely replicate the conditions of the experiment we recalculated the enhancement factor this time comparing the resonant peak value to the nonresonant signal in the ER configuration [approach (c)]. In performing this calculation we used the experimental values for the incident and scattering angles in the ER case. However, we were restricted to using the backscattering configuration (instead of the actual experimental scattering of 120° on the ring) for the resonant case. For arbitrarily equal ripple amplitudes for the different phonon frequencies in the two configurations, we calculate an enhancement factor of 800. The increase from the value of 415 calculated above is attributable to the fact that one nonresonant scattering calculation is for the Ag-glass interface and the other for the Ag-air interface, involving different mismatching of the dielectric constants. In addition, the incident and scattering angles differed appreciably for the two calculations.

The calculated enhancement value of 800 is in good agreement with the value of 750 determined experimentally, even though (i) the in-plane scattering condition of the calculation does not match the out-of-plane condition of the measurements, and (ii) the experimental determination could not be made at the very peak intensity on the thin ring of scattered light. We would expect that the experimental value thus obtained should be less than its optimum.

As in the experimental comparison of enhancement for cases (1) and (2), the theory gives a value much larger for case (1) than for case (2), specifically, 800 and 25, respectively. The greater enhancement is for the case where the resonant interaction of SP's occurs twice, for both the incident and scattered light.

V. COMPARISON WITH SP ENHANCED RAMAN SCATTERING

We have reported here an enhancement by a factor of the order of 1000 for Brillouin scattering on smooth Ag films, with the enhancement determined purely by the involvement of propagating SP's. The magnitude of the enhancement is very sensitive to the value of the dielectric constant of the Ag film. It is of interest to compare our results with those available in the literature for Raman scattering, which is the closest in concept of the various enhanced nonlinear optical phenomena.

To maintain conditions for the comparison as identical as possible, we should consider only the case of the Kretschmann ATR configuration, with a *monolayer* of chemical adsorbate on a *smooth* Ag film. Smooth films ensure that the enhancement is due to propagating SP's, as opposed to roughened surfaces where the SP's are localized and enhancement factors may be much larger. However, we are not aware of any reports in the literature of measurements of the enhancement of Raman scattering for exactly the desired conditions. What has been reported involves various subterfuges in order to obtain measurable signals for the unenhanced and/or enhanced Raman signals. We consider two examples below.

One approach involved slight electrochemical roughening of the surface to obtain an initially measurable Raman signal from adsorbed molecules in the ER configuration. The additional enhancement that comes from using propagating SP's in the Kretschmann ATR configuration can then be determined by passing the light through the prism. For the forward scattering configuration corresponding to our case (2), additional enhancement factors between 5 and 10 have been reported[12,13] This is appreciably lower than our value of 25. Such a reduced enhancement factor is not surprising. For the roughened surfaces, the reflectivity dip corresponding to SP resonance was reported to be broadened, indicating a change in dielectric constant, particularly an increase in the imaginary component.

A second approach employed a large volume of the Raman active agent—instead of a monolayer—in contact with the Ag film. The amplitude of the electric fields of the SP's decay exponentially away from the surface of plasmon generation and the enhanced Raman signal is due to the large number of molecules within this decay length. The unenhanced Raman signal is taken separately from a bulk solution of the chemical species. The calculation of the enhancement factor is then dependent on the estimated ratio of the scattering volumes for the two cases. Ushioda and Sasaki[14] obtain a "rough estimate" for the SP enhancement of 4×10^4 for the case of resonant scattering on the prism side of the film, corresponding to our case (1). Since the dielectric constant of the Ag film was not measured in this experiment, the enhancement factor cannot be compared with theory.

There also seems to be little consensus for theoretical calculations of the enhancement factor for Raman scattering. Chen *et al.*[15] obtained an enhancement of ~ 100 for forward scattering on the air side as in case (2), with an additional enhancement of only 3 or 4 for backscattering through the prism, as in case (1). A contrasting analysis by Sakoda *et al.*[16] stressed the double enhancement factor in case (1). They obtained an enhancement factor of 150 for the resonant coupling of the incident light to SP's, and an additional factor of 290 for the resonant coupling in the Raman scattered light. The net enhancement for case (1) is then about 4×10^4. The dielectric constant of the Ag film assumed in this analysis is $-10.79+i0.33$, which should give a higher enhancement than we determined for case (1) for Brillouin scattering, but not enough to give the factor-of-50 greater enhancement.

VI. CONCLUSION

In this paper, we have analyzed and quantitatively determined the SP-induced enhancement of surface Brillouin scattering from phonons of a thin Ag film in a Kretschmann ATR configuration. The emphasis in this paper was on the backscattering configuration in which the SP resonance is doubly involved, i.e., in both the incident and scattered light. Previous theoretical analysis predicted that the Brillouin cross section would be greatly enhanced for such a scattering process. By considering the conservation conditions governing the interaction between light and SP's, we have shown that the doubly resonant Brillouin scattered light emerging back through the prism is confined to the shell of a cone. The resulting enhancement in the Brillouin scattering cross section was measured by comparing the Brillouin scattered intensity from light on the cone to that for the ER configuration in which there is no SP participation. The measured enhancement value of 750 was much greater than the value of 25 determined previously for the single involvement of SP's. To make a quantitative comparison with theoretical predictions we adapted the theory of Marvin *et al.*[11] to numerically calculate the enhancement factor. For a configuration that resembled (but was not identical to) that used experimentally, we calculated an enhancement factor of 800, in good agreement with our measurement. There were a number of factors and corrections both in the measurement and in the calculation that have to be carefully analyzed to obtain the quoted enhancement values, and these were dealt with in detail in the paper.

To place our measurement of enhancement in context

we reviewed the literature for similar attempts using Raman scattering from adsorbates. Such experiments suffered from the difficulty of measuring the weak Raman signals from molecular monolayers, particularly for the unenhanced case, and various subterfuges had to be employed. We can conclude that Brillouin scattering offers a distinct advantage since both the enhanced and unenhanced signals could be directly measured. In addition, the confinement of the ripples of the acoustic waves to the surface meant that they were ideal candidates for probing the peak fields of the SP's.

We have emphasized that the SP enhancement factor depends strongly on the conditions under which the experiment is performed. Our experiments demonstrate the very different enhancement values obtained for the forward and backward scattering configurations. In addition, the enhancement value is very sensitive to the imaginary part of the dielectric constant which is, from our experience, strongly dependent on the surface quality of the metal film. This sensitivity of the enhancement to the material properties means that it is only possible to properly analyze data for which the dielectric constant of the particular film is measured.

In terms of a practical technique for increasing surface Brillouin scattering cross sections this method has a number of limitations. It is restricted to thin films and to materials that support SP's, notably the noble metals. The thin-film restriction could be overcome by working in the Otto[17] geometry. However, more importantly, our work serves as a powerful adjunct to the numerous experiments that have attempted to characterize the role of SP's in enhancing surface optical processes.

ACKNOWLEDGMENTS

The work was supported by the National Science Foundation through the Materials Research Laboratory Program Grant No. DMR-80-20249, and equipment support from Grant No. 82-17442. One of the authors (R.B.) gratefully acknowledges assistance from the von Humboldt Foundation during part of the preparation of this manuscript.

*Present address: Amoco Research Center F4 P.O. Box 400, Naperville, IL 60566.

[1]For reviews, see *Surface Enhanced Raman Scattering,* edited by R. K. Chang and T. E. Furtak (Plenum, New York, 1982); A. Otto, K. Arya, and R. Zeyher in *Light Scattering in Solids IV,* Vol. 54 of *Topics in Applied Physics,* edited by M. Cardona and G. Güntherodt (Springer-Verlag, Berlin, 1984).

[2]H. J. Simon, D. E. Mitchell and J. G. Watson, Phys. Rev. Lett. **33**, 1531 (1974).

[3]Y. R. Shen, in *Novel Materials and Techniques in Condensed Matter,* edited by G. W. Crabtree and P. Vashishta (Elsevier, New York, 1982).

[4]A. L. Moretti, W. M. Robertson, B. Fisher, and Ralph Bray, Phys. Rev. B **31**, 3361 (1985).

[5]S. Mishra and R. Bray, Phys. Rev. Lett. **39**, 222 (1977).

[6]R. Loudon and J. R. Sandercock, J. Phys. C **13**, 2609 (1980).

[7]H. J. Simon and J. K. Guha, Opt. Commun. **18**, 394 (1976).

[8]A. J. Braundmeier, Jr. and H. E. Tomaschke, Opt. Commun. **14**, 99 (1975).

[9]H. Raether, in *Surface Polaritons,* edited by V. M. Agronovich and D. L. Mills (North-Holland, Amsterdam, 1982).

[10]M. Fukui, O. Toda, V. C. Y. So, and G. I. Stegeman, Solid State Commun. **36**, 995 (1980); J. Phys. C **14**, 5591 (1981).

[11]A. Marvin, V. Bortolani, F. Nizzoli, G. Santoro, and V. Celli, J. Phys. C **15**, 3273 (1982).

[12]B. Pettinger, A. Tadjeddine, and D. M. Kolb, Chem. Phys. Lett. **66**, 544 (1979).

[13]H. W. K. Tom, C. K. Chen, A. R. B. de Castro, and Y. R. Shen, Solid State Commun. **41**, 259 (1982).

[14]S. Ushioda and Y. Sasaki, Phys. Rev. B **27**, 1401 (1983).

[15]Y. J. Chen, W. P. Chen, and E. Burstein, Phys. Rev. Lett. **36**, 1207 (1976).

[16]K. Sakoda, K. Ohtaka, and E. Hanamura, Solid State Commun. **41**, 393 (1982).

[17]A. Otto, Z. Phys. **241**, 313 (1971).

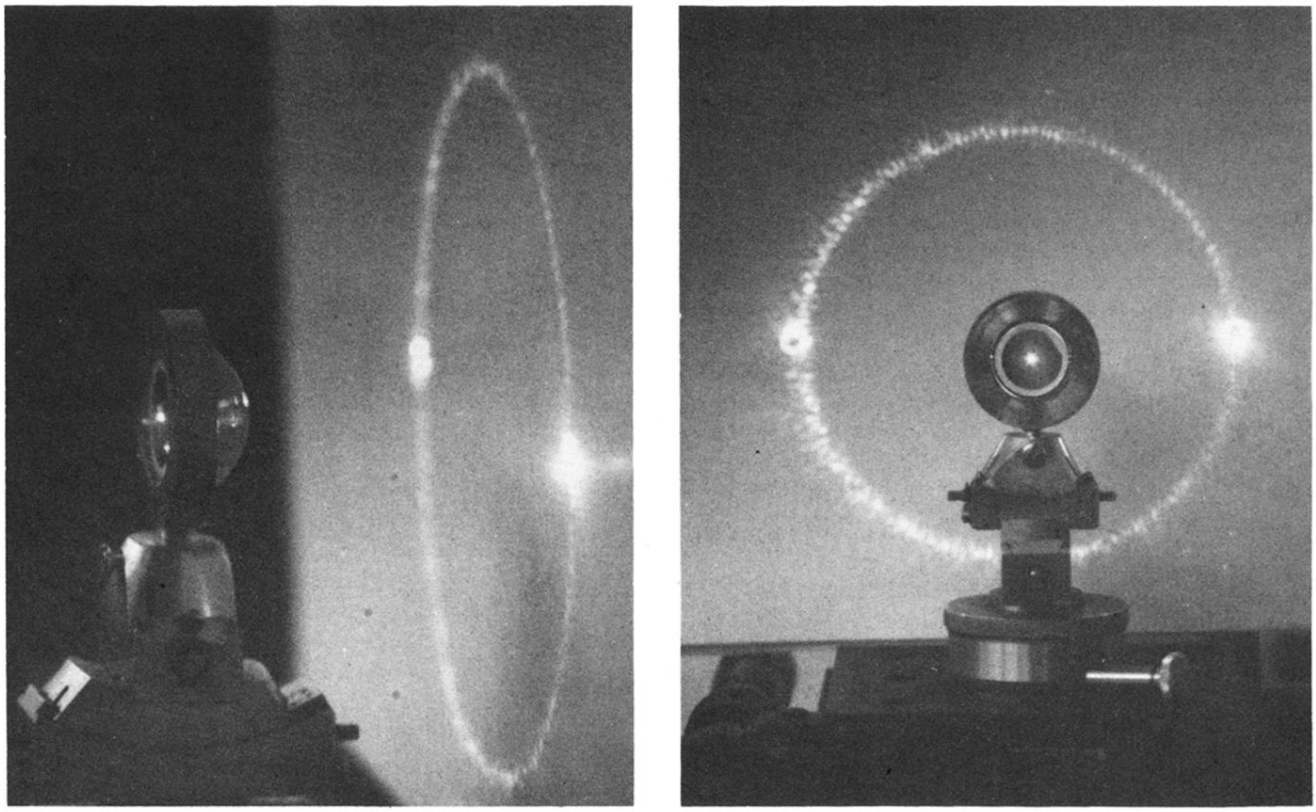

FIG. 2. Photographs with front and side views of the experimental configuration showing the ring of light projected on a screen; the ring is due to SP wave-vector randomization by scattering in the Ag film and subsequent reradiation through the glass via prism coupling.